The magnetism of UX_3 compounds (X = In, Pb, Ga) from symmetry considerations and perturbed-angular-correlation spectroscopy

2000 J. Phys.: Condens. Matter 12 4629

(http://iopscience.iop.org/0953-8984/12/21/307)

J. Phys.: Condens. Matter **12** (2000) 4629–4639. Printed in the UK PII: S0953-8984(00)10316-9

The magnetism of UX_3 compounds (X = In, Pb, Ga) from symmetry considerations and perturbed-angular-correlation spectroscopy

S Demuynck†, L Sandratskii‡, S Cottenier†, J Meersschaut† and M Rots†

† Instituut voor Kern- en Stralingsfysica, KU Leuven, Celestijnenlaan 200D, B-3001 Leuven, Belgium

‡ Institut für Festkörperphysik, Technische Universtität Darmstadt, Hochschulstrasse 6/8, D-64289 Darmstadt, Germany

E-mail: steven.demuynck@fys.kuleuven.ac.be

Received 13 December 1999, in final form 29 February 2000

Abstract. We show how symmetry considerations and *ab initio* calculations within the framework of the density-functional theory can be used in the analysis of the appearance and orientation of magnetic hyperfine fields. This approach, in which the incorporation of spin–orbit coupling is essential, provides information about hyperfine fields also for the sites where the Heisenberg exchange field is zero. This is of crucial importance in the interpretation of magnetic hyperfine-field measurements. We apply this theoretical scheme and perturbed-angular-correlation experiments to study the magnetic structure of UX_3 compounds with X = Ga, In, Pb. For UPb_3 we find a triaxial structure with U moments along the [111] axes. In UIn_3 the U moments are arranged in a type-II antiferromagnetic structure with moments along [110].

1. Introduction

Hyperfine fields arise from the interaction between the nucleus and its surrounding electron cloud. In magnetic solids this cloud is spin polarized. Through the interatomic interaction the polarization involves also the states of diamagnetic atoms. On the nucleus of a diamagnetic atom, this induced spin polarization leads to a hyperfine field of transferred nature. As a first estimate of the magnitude and direction of this hyperfine field one commonly relies on the vector sum of the nearest-neighbour magnetic moments. This simple guess, based on the Heisenberg exchange Hamiltonian, has proven to be successful in many cases. However, in the case where the Heisenberg exchange field on the site of the nucleus is zero, adjustments to the inducing magnetic structure or secondary effects like magnetostriction are usually invoked to explain the appearance of magnetic hyperfine fields. In this work we provide a more fundamental approach to this problem.

There are three contributions to the hyperfine field, of which the Fermi-contact term is the most important one. The dipole term and the contribution from the orbital moment can be neglected in a first approximation. The Fermi-contact term stems from the contact field originating from s electrons penetrating into the nucleus. If there is a net spin density at the nucleus, a hyperfine field arises. The s spin density at the nucleus is roughly proportional to the s spin moment of the atom. Hence an induced s spin moment on a non-magnetic atom

0953-8984/00/214629+11$30.00

will result in a finite magnetic hyperfine interaction between the nucleus of this atom and its electron states.

The present calculation method is based on the local density approximation to the density-functional theory of itinerant-electron systems. It is generalized to the case of non-collinear magnetism and takes into account the effect of spin-orbit coupling (SOC) which makes it especially suitable for the study of U compounds [1]. Important information on the appearance and orientation of magnetic moments can be gained immediately from the investigation of the symmetry of the Hamiltonian of the problem.

We use this method to interpret our measurements of magnetic hyperfine fields in UX_3 compounds with X = Ga, In, Pb and to determine their magnetic structure. A number of magnetic configurations have been proposed in the literature. Our purpose is to select for each of the compounds the structure which is in the best agreement with our theoretical and experimental results. Most of the information on the magnetism of UX_3 compounds has so far been obtained by means of neutron diffraction studies on polycrystalline samples. For UPb_3, neutron diffraction cannot be used to distinguish between the magnetic unit cells corresponding

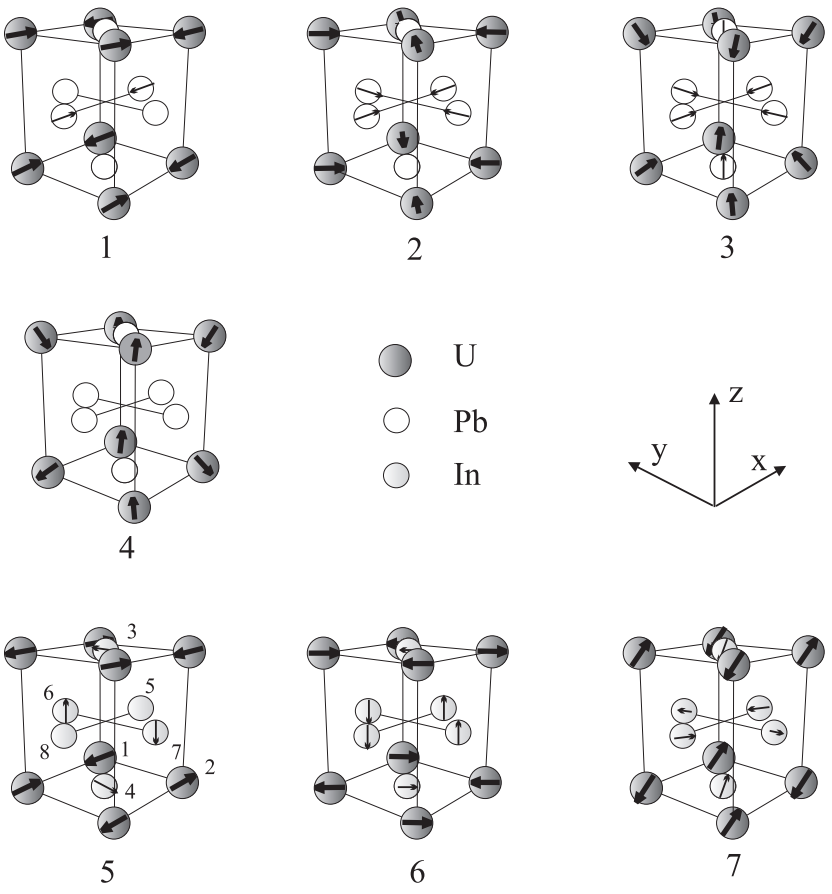

Figure 1. Models for the magnetic structure of UPb_3 and UIn_3 (UGa_3) developed on the basis of neutron diffraction results. The direction of the electric field gradient is always perpendicular to the cubic side planes. The induced magnetic moments and hyperfine fields on Pb and In(Ga) sites are shown. The eight positions discussed in the symmetry analysis of structure 5 are indicated.

to a monoaxial AFI[100], a biaxial and a triaxial (NdZn) structure, as indicated in figure 1 [2,3]. In further discussion, we label these structures as 1, 2 and 3 respectively. Another triaxial structure can be proposed on the basis of the neutron diffraction data. This magnetic structure has been established for $TbIn_3$ [4] and will be called structure 4. The indeterminacies of the size of the magnetic unit cell and the absolute moment directions are inherent to neutron diffraction studies on polycrystals.

For UIn_3 and UGa_3 a type-II antiferromagnetic structure (AFII) is proposed, but again no information on the absolute orientation of the moments is available [5, 6]. One can expect the moments to be parallel to one of the three main crystallographic axes: [100], [110] and [111]. The corresponding magnetic structures will be numbered as structures 5, 6 and 7.

Because the neutron diffraction by polycrystalline samples of these compounds does not allow one to identify uniquely their magnetic structures, the use of experimental techniques providing complementary information about the magnetic structure is essential. Mössbauer studies using ^{119}Sn probes on UPb_3 and UIn_3 report the presence of a large hyperfine field on Sn in the Pb position and a small hyperfine field on Sn in the In position. Unfortunately, the interpretation of the Mössbauer data is also not unambiguous [7–10]. Recently, a perturbed-angular-correlation (PAC) study of UIn_3 indicated that a modification to the simple AFII structure was needed to explain the measured spectra [11].

2. Symmetry analysis

In order to explain why the induced moments and hyperfine fields on the X atoms appear and orient in a particular way, we turn now to a symmetry analysis of the magnetic structures collected in figure 1. The present analysis is based on principles that have been reviewed extensively in [1, 12]. In [12] a symmetry criterion has been suggested for the appearance of an induced moment on a non-magnetic atom in a magnetic crystal. Adapted to the case of UX_3 compounds, this criterion can be formulated as follows. *The induced magnetic moments on the X atoms cannot break the symmetry of the inducing U sublattice*. Thus, by studying the transformations that leave the U magnetic structure invariant, we can draw conclusions about the possible directions of the induced magnetic moments. If any orientation of the moments of the X atoms disturbs at least one of the symmetry operations of the U magnetic structure, no induced magnetic moments can appear. As opposed to this, if the appearance of magnetic moments on the X atoms does not disturb the symmetry of the inducing structure, these moments must appear because the probability of a non-magnetic state for the X atoms is in this case negligible [12].

Note that the results of the symmetry analysis are different for relativistic and non-relativistic problems since these problems are described by different groups of symmetry operations [1]. In a non-relativistic case it is a spin-space group which allows different transformations of spin and space variables. In a relativistic case it is a usual space group with identical transformations of spin and space variables. Since for the U compounds SOC plays an essential role, the present symmetry analysis is based on the space groups.

As an example we show how symmetry determines the In-sublattice magnetism in UIn_3 with U moments oriented along [100] (structure 5). The generators of the group of symmetry operations that leave the U-sublattice magnetism invariant are summarized in table 1. The operations C_{2z} and C_{2y} do not change the positions of atoms 5 and 8. Then from the third column of table 1 it follows that any moment on these atoms will destroy the symmetry with respect to at least one of these operations. Hence, no induced moment can appear on these atoms. Operation C_{2y} does not change the positions of atoms 3 and 4 and transforms m_z into $-m_z$ and m_x into $-m_x$. Therefore, according to this symmetry operation the magnetic moment

Table 1. The first column shows the generators of the symmetry group of the U-sublattice magnetization of UIn_3 with magnetic structure 5. C_{2z} is a rotation around the z-axis by 180°, C_{2y} is a rotation around the y-axis and R is the time-reversal operator. The non-primitive translations accompanying some of the operations are also shown in the table. The third column shows the effect on an axial vector, where i and j indicate the transposition of atoms as indicated by column 2.

Operation	Transposition of atoms	Restrictions on magnetic moments
$C_{2z}[100]$	$\begin{pmatrix} i & 1 & 2 & 3 & 4 & 5 & 6 & 7 & 8 \\ j & 2 & 1 & 4 & 3 & 5 & 6 & 7 & 8 \end{pmatrix}$	$\begin{pmatrix} m_x \\ m_y \\ m_z \end{pmatrix}_i = \begin{pmatrix} -m_x \\ -m_y \\ m_z \end{pmatrix}_j$
C_{2y}	$\begin{pmatrix} i & 1 & 2 & 3 & 4 & 5 & 6 & 7 & 8 \\ j & 2 & 1 & 3 & 4 & 5 & 7 & 6 & 8 \end{pmatrix}$	$\begin{pmatrix} m_x \\ m_y \\ m_z \end{pmatrix}_i = \begin{pmatrix} -m_x \\ m_y \\ -m_z \end{pmatrix}_j$
$R[100]$	$\begin{pmatrix} i & 1 & 2 & 3 & 4 & 5 & 6 & 7 & 8 \\ j & 2 & 1 & 4 & 3 & 8 & 7 & 6 & 5 \end{pmatrix}$	$\begin{pmatrix} m_x \\ m_y \\ m_z \end{pmatrix}_i = \begin{pmatrix} -m_x \\ -m_y \\ -m_z \end{pmatrix}_j$

on these atoms can arise only in the y-direction. Since other operations impose restrictions only on the *relative* directions of the moments of atoms 3 and 4, they allow the appearance of induced moments on these atoms. As stated above, if none of the symmetry operators is destroyed by the appearance of induced moments, these moments must appear. Thus we can conclude that there are induced moments on atoms 3 and 4, collinear with the y-axis and antiparallel to each other. Similar arguments apply to atoms 6 and 7. A finite magnetic moment must develop on these atoms. These moments are collinear with the z-axis and antiparallel to each other.

Similar arguments help to explain the features of the other configurations of UIn_3 and UPb_3, summarized in figure 1. The corresponding symmetry operations are given in table 2. In structure 6 for UIn_3, induced moments should appear on all In sites. They are oriented parallel to the side planes of the cube (figure 1). The AFII structure with magnetic moments along the [111] axes (structure 7) appeared to be unstable. This structure is not distinguished by symmetry from the structures with moments deviating from the [111] directions. In the calculations the moments deviate from the [111] axes tending to assume accidental directions supplying the minimum in total energy. Self-consistent determination of the accidental directions of the magnetic moments is very time consuming and has not been carried out.

Table 2. Generators of the symmetry group of the U-sublattice magnetization for the magnetic structures indicated in figure 1. The meanings of the operator symbols are as in table 1. I stands for the inversion operator. Non-primitive translations accompanying some of the operators are also included.

Structure	Generators
1	C_{4x}, I, $C_{2y}[100]$, $R[100]$
2	$C_{2x}[011]$, $C_{4z}[010]$, I, $R[111]$
3	$C_{4x}[010]$, $C_{4y}[001]$, $C_{3[111]}$, I, $R[111]$
4	$C_{2x}[011]$, $C_{2y}[101]$, $C_{3[111]}$, I, C_{4z}, $R[101]$
5	$C_{2z}[100]$, C_{2y}, $R[100]$
6	$C_{2[x=-y]}$, $C_{2z}[100]$, I, $R[100]$
7	$C_{2[x=y]}[100]$, I, $R[100]$

In UPb_3, all Pb magnetic moments are directed normal to the side planes of the cube

(figure 1). For structure 1, we have two thirds with a zero moment and one third with a finite moment. In structure 2, the situation is opposite: two thirds of the Pb atoms have a finite moment and one third have a zero moment. While in structure 4 none of the Pb atoms has a moment, each of them has a finite moment in structure 3.

Since structures 5, 6 and 7 were also proposed for UGa_3, the results from the symmetry analysis for UIn_3 also apply to that case.

3. *Ab initio* calculations

The Hamiltonian used in the calculations contains SOC and the orbital polarization term $\hat{H}_{orb} = I_{orb} L\hat{l}$ that accounts for Hund's second rule, with L the atomic orbital moment, $\hat{l}$ the angular momentum operator and I_{orb} the orbital polarization parameter. A more detailed description of the Hamiltonian can be found elsewhere [1]. The actual calculations were done by the augmented-spherical-wave (ASW) method. Within the ASW method, one requires the atomic-sphere approximation (ASA). Space is filled with almost non-overlapping spheres associated with U and X atoms. The charge transfer for the choice made is always less than 0.1 electrons/atom. All calculations are performed with 64 k-points in the unit cell.

3.1. UPb_3

For the sake of better comparison, we have performed calculations of the four proposed magnetic structures using the same unit cell. This unit cell is cubic with a lattice parameter that is twice the crystallographic lattice parameter. The unit cell contains 8 U atoms and 24 Pb atoms. Because of the large number of atoms per unit cell, the calculations were very time consuming. From a density-of-states calculation performed with the FLAPW package WIEN97 [13], we assessed the importance of the unpopulated 5f Pb states to be negligible, so they are left out of the calculation. We started calculations with non-magnetic Pb atoms. In full agreement with the symmetry analysis, some of the Pb atoms obtained an induced magnetic moment, while some remained in the non-magnetic state. Also, the directions of the induced moments are in agreement with the predictions of the symmetry analysis. Table 3 summarizes the induced s spin moments on the Pb atoms for the four magnetic structures. In the total magnetic unit cell of structure 3, obtained by doubling the cell of figure 1 in all directions, we recognize two fractions having different induced spin moments. At the origin of this lies a difference in U-magnetic-moment surroundings. Half of the Pb atoms are surrounded by U atoms with magnetic moments pointing towards the centre of the same cube, while for the other half of the Pb atoms the U moments point towards centres of different cubes.

3.2. UIn_3

The UIn_3 neutron diffraction measurements convincingly established the magnetic ground state to be AFII. The U moments in UIn_3 are known to be collinear but their direction with respect to the crystal lattice is unknown. The calculations for UIn_3 are easier than for UPb_3, since a smaller magnetic unit cell with only two U atoms and six In atoms can be used.

The results are summarized in table 4 and figure 1. Again, the calculated induced spin moments confirm the results of the symmetry analysis. In structure 5, atoms 3 and 4 have a different spin moment to atoms 6 and 7. Also, in structures 6 and 7, two fractions with different induced spin moments can be distinguished.

Table 3. Induced s spin moments on Pb atoms for the different Pb positions in, and the magnetic structures proposed for UPb_3. Figure 1 does not show the full magnetic unit cell. The two numbers indicated for structure 3 result from inequivalent Pb atoms in the total magnetic unit cell.

	Induced s spin moment (10^{-3} μ_B)		
UPb_3 structure	Pb (3, 4)	Pb (5, 8)	Pb (6, 7)
1	0	4.2	0
2	0	5.2	5.2
3	4.1	4.1	4.1
	5.3	5.3	5.3
4	0	0	0

Table 4. Induced s spin moments on the different In positions in, and the different magnetic structures proposed for UIn_3.

	Induced s spin moment (10^{-3} μ_B)		
UIn_3 structure	In (3, 4)	In (5, 8)	In (6, 7)
5	0.06	0	0.09
6	2.4	0.31	0.31
7	1.2	0.67	0.67

Note that if SOC is neglected, the magnetic structures 5, 6 and 7 are equivalent. Therefore, the differences in values for the induced moments on the In atoms (table 4) are a consequence of SOC, creating differences in the interatomic interactions.

Calculations show that the conclusions on the appearance and orientation of the induced moments in UIn_3 also hold in the case of UGa_3.

3.3. Discussion

The calculations of the induced s spin moments on the Pb, In and Ga atoms are by no means predictions for the magnetic hyperfine field on the ^{111}Cd impurity nucleus, used in PAC experiments. However, all predictions concerning the appearance and orientation of induced s spin moments and thus magnetic hyperfine fields are equally valid, assuming the Cd impurity on an X position does not alter the U magnetic structure.

In the case of UPb_3, the directions of the induced moments and thus the induced hyperfine fields, as derived from the symmetry analysis and calculations, correspond to the expectations based on the Heisenberg model. It can be shown that in all cases where the vector sum of the nearest-neighbour magnetic moments is non-zero, the appearance of the induced magnetic moments does not break the symmetry of the magnetic sublattice. Therefore, the induced moments must appear. This explains why the Heisenberg model works well in many cases. In UIn_3 on the contrary, at each In position the vector sum of the magnetic moments of nearest-neighbour U atoms is zero. This, however, does not mean that no hyperfine field will arise on the In position. The symmetry analysis has to be performed in that case. If a symmetry-preserving direction is found, the induced magnetic moment must appear. Here it is important to stress that the result of the symmetry analysis can differ, depending on whether SOC is included or not. In the analysis of the structures reported on, SOC is taken into account. To demonstrate the possible difference: note that in the non-relativistic case the magnetic moment induced by a collinear magnetic structure is always collinear with the inducing moments. As

a consequence, in structures 5, 6 and 7 no induced moments would appear.

The interpretation of transferred magnetic hyperfine fields on diamagnetic probe nuclei in general should therefore consider the symmetry of the inducing magnetic structure including SOC, especially on sites where the Heisenberg exchange field is zero.

The preceding theoretical study has provided us with models for analysing the magnetic hyperfine fields on diamagnetic ^{111}Cd probes substituted into X positions for the different structures proposed.

4. Experimental results

The samples were prepared by conventional arc-melting techniques at the Institute for Transuranium Elements, Karlsruhe. Because of their extreme sensitivity to moisture and oxygen, they were constantly kept in vacuum or in a protective Ar atmosphere. Trace quantities of the radioactive probe ^{111}In were introduced into the sample by diffusion for 20 h at 700 °C. The samples were powdered prior to every measurement to remove any texture effects. The ^{111}In nuclei decay with a half-life of 2.83 days into an excited state of ^{111}Cd. In the further decay to the ^{111}Cd ground state, a γ–γ cascade is encountered with a half-life of 80 ns for the isomer. The PAC method is essentially the measurement of that lifetime, by detecting in time coincidence both γ-rays in a four-detector set-up with 90°/180° inter-detector angles. In the presence of an electric field gradient and/or a magnetic hyperfine field at the probe position, well-known oscillations superimpose on this lifetime. A mathematical operation with spectra obtained from different detector combinations removes the exponential decay and highlights the oscillations. This is the PAC anisotropy time spectrum or $R(t)$ spectrum. This $R(t)$ spectrum contains information on the strength, orientation and asymmetry of the perturbing extranuclear fields. The Cd probe atom is diamagnetic, which makes all magnetic hyperfine fields purely transferred. Extra details on the experimental technique [14] and the program used for the analysis [15] can be found elsewhere.

4.1. UPb_3

In measurements above the magnetic ordering temperature ($T_N = 32$ K), the observation of an electric field gradient reveals information on the site location of the probe. The spectrum shown in figure 2 is characteristic of a single and axially symmetric electric field gradient. As the Pb site, compared to the U site and interstitial sites, is the only one with a non-cubic

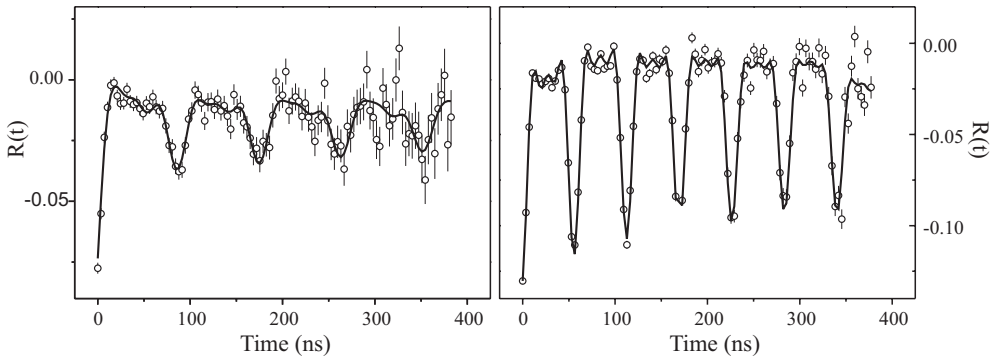

Figure 2. PAC time spectra at room temperature for (left) UPb_3 and (right) UIn_3.

and axially symmetric surrounding, this proves that the probes diffuse mainly into the Pb positions. The three electric field gradients, as expected from the local environment, with their principal axes oriented perpendicular to the (001), (010) and (100) planes respectively, are equivalent due to the randomness in a polycrystal. The magnitude V_{ZZ} of the electric field gradient is derived from the precession frequency by using $\nu = eQV_{ZZ}/h$ with Q the quadrupole moment of the probe. Above T_N, V_{ZZ} scales linearly with temperature (slope $= -(2.27 \pm 0.15) \times 10^{-4}$ K^{-1}); this is a common feature for f-electron materials, but not understood yet [16, 17]. The loss of anisotropy in the first part the spectrum, as compared to the UIn_3 case (figure 2), points towards an ill-defined environment for a sizable fraction of the probes. This is presumably related to Pb clusters inside the sample.

Below T_N, the U moments polarize the conduction electrons of the probe leading to a finite spin density at the diamagnetic probe nuclei. Then, the probes experience a combined hyperfine interaction with an electric field gradient and a transferred magnetic hyperfine field. Depending on the magnitude and orientation of the hyperfine-field axis relative to the electric field gradient principal axis, characterized by the angle β, it is possible to distinguish between the proposed models for the magnetic structure. At this point, the symmetry analysis and calculated spin magnetic moments are used to construct models for analysing the experimental spectra. They determine the occurrence of a hyperfine field and predict the angle β. As such we get good starting parameters for the analysis of the PAC spectra.

The result of the analysis of a spectrum at 25 K is shown in figure 3. Structure 4 is not included, since a model with no hyperfine fields should resemble the measurement at room temperature. This is clearly not the case, so we can immediately exclude this model. It is clear that structure 3 applies best as regards fitting the experimental spectra. We use indeed a fit model with all probes experiencing a combined interaction, half of which are subject to a slightly larger hyperfine field. The preference for structure 3 is systematic at all temperatures and for all samples measured. The measured magnetic hyperfine fields at 25 K are 2.71(2) T

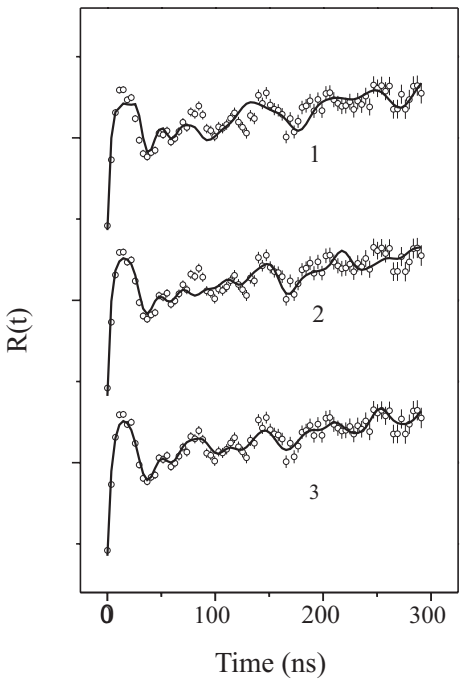

Figure 3. PAC time spectra on UPb_3 at 25 K, fitted with three models for the structures indicated.

and 2.04(1) T respectively. In this case the ratio for the calculated induced s spin moments on the two types of Pb atom is relatively close to the ratio of magnetic hyperfine fields on ^{111}Cd in these positions.

4.2. UIn_3

The probe site location found in UIn_3 is the same as in UPb_3: the ^{111}In parent probe, not being an impurity, diffuses almost entirely into an In position. Also, the fraction at In clusters is very small. This explains the less damped spectrum for UIn_3 above T_N (figure 2). Also here, the principal axes of the electric field gradients are oriented perpendicular to each of the side planes of the cube.

In a previous PAC study of UIn_3 [11], it was immediately clear that at least a proportion of the probes were subject to a magnetic hyperfine field. Small deviations from the simple AFII structure like changes in the U-moment magnitude or tilting the moments over a small opposite angle were needed to explain the appearance of magnetic hyperfine fields. Both these adjustments equally supported the interpretation of the experimental patterns based on two sites: one third with their hyperfine fields oriented parallel, the other two thirds perpendicular to the local electric field gradient principal axis.

To pinpoint the details of the proposed magnetic structure, new spectra with very high statistical accuracy were taken at 4.2 K. The model for the magnetic structure from [11] failed to fit these high-precision data. The symmetry analysis of section 2 made it clear that it is indeed the case that no changes in the U-moment magnitude or tilting are needed to explain the magnetic hyperfine fields. Moreover, for the different magnetic structures, this analysis yields important information on the magnetic hyperfine-field appearance and its relative orientation with respect to the electric field gradient. Figure 4 shows the fits resulting from the three models applied. A crucial feature in the fits is the allowance for a non-axially symmetric electric field gradient on the In sites: the fourfold crystalline axial symmetry is broken by the induced hyperfine field. While structure 7 clearly cannot account for the experimental pattern, the differences between structures 5 and 6 are very small. In the two models the magnetic hyperfine fields are oriented perpendicular to the principal axes of the electric field gradient,

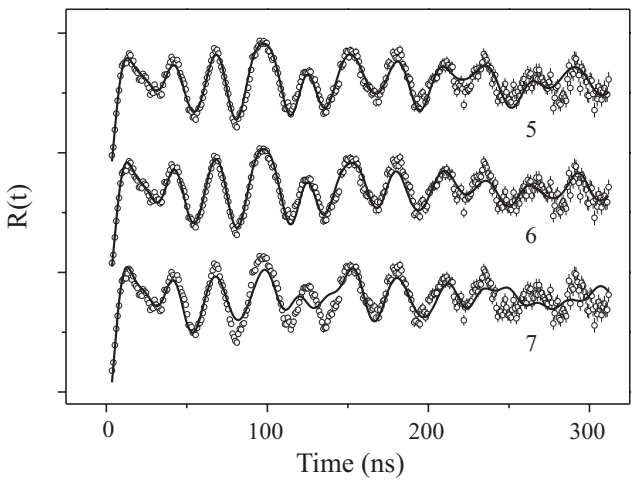

Figure 4. High-statistics PAC time spectra on UIn_3 at 4.2 K, fitted with models for the three structures indicated.

but in structure 5 one third of the probes experience the electric field gradient only. Because the strengths of the two hyperfine interactions are similar, this does not lead to major differences in the simulated spectra for structures 5 and 6. However, a careful analysis reveals that the simulation for structure 6 fits the data more closely. It also constitutes a clear improvement with respect to the analysis in [11] at all temperatures below T_N. The measured hyperfine fields on ^{111}Cd in an In position at 4.2 K are 1.48(1) T and 1.07(1) respectively. The presence of two different magnetic hyperfine fields confirms the predictions of the symmetry analysis and calculations for structure 6. However, the calculated s spin moments on In clearly do not constitute a prediction of the relative magnitude of the magnetic hyperfine fields on the ^{111}Cd nuclei.

Also, in the interpretation of recent NQR spectra of $CeIn_3$ for which neutron diffraction study revealed the same AFII structure, with no information on the absolute magnetic moment orientation, as for UIn_3 [18], small transferred hyperfine fields are found oriented perpendicular to the local electric field gradient principal axes [19]. For both UIn_3 and $CeIn_3$, we can now establish structure 6 to be the magnetic structure.

4.3. UGa_3

We have also tried to perform PAC measurements on UGa_3. Attempts were made to diffuse the ^{111}In parent probe into the Ga positions at various annealing temperatures. Ion implantation followed by different annealing steps was unsuccessful as well. Apparently the annealing procedure produces large Ga clusters, since the electric field gradient observed by the ^{111}Cd probes is reminiscent of that of α-Ga [20]. We can therefore not deduce the magnetic ordering with the PAC technique as we could for UPb_3 and UIn_3.

5. Conclusions

We have shown that symmetry considerations and calculations of the induced s spin moment, incorporated in the analysis of magnetic hyperfine fields, can give much more reliable information on the appearance and orientation of the field as compared to the crude estimation from a vector sum of the magnetic moments of nearest neighbours. The PAC measurements on UIn_3 and the NQR measurements on $CeIn_3$ reveal a hyperfine field, at sites where the Heisenberg exchange field is zero. They confirm the predictions based on symmetry considerations. To our knowledge, these observations are the first in which the features of purely transferred magnetic hyperfine fields are interpreted as arising from effects other than exchange.

The present theoretical approach selects magnetic structure models for analysing the experimental PAC spectra. In our study of the magnetic structure for UX_3 compounds, we find evidence for a triaxial magnetic structure with moments along the [111] directions in UPb_3. In UIn_3, a simple AFII structure with moments along the [110] directions explains the experimental spectra in all their details, in contrast to modifications suggested in [11]. This magnetic structure is now also established for $CeIn_3$. For technical reasons the present experimental approach was not feasible for UGa_3. Since UGa_3 is the only UX_3 material up to now for which single crystals can be grown successfully, a neutron diffraction study would be very useful here. We predict it to have the same magnetic structure as found here for UIn_3.

Acknowledgments

We are indebted to Dr J C Spirlet and Dr D Kaczorowski for providing the samples. SC is a Postdoctoral Fellow of the Fund for Scientific Research—Flanders (FWO). LS acknowledges the support of the Deutsche Forschungsgemeinschaft through Sonderforschungsbereich No 252. This work was financially supported by the FWO 95.0137.95 project and the 'Vlaamse Wetenschappelijke Stichting'

References

[1] Sandratskii L M 1998 *Adv. Phys.* **47** 91–160
[2] Leciejewicz J and Misiuk A 1972 *Phys. Status Solidi* a **13** K79–81
[3] Murasik A and Zolnierek Z 1980 *Physica* B **98** 306–10
[4] Galéra R M, Amara M, Morin P and Burlett P 1998 *J. Phys.: Condens. Matter* **10** 3883–902
[5] Murasik A, Leciejewicz J, Ligenza S and Misiuk A 1973 *Phys. Status Solidi* a **20** 395–401
[6] Lawson A C, Williams A, Smith J L, Seeger P A, Goldstone J A, O'Rourke J A and Fisk Z 1985 *J. Magn. Magn. Mater.* **50** 83–7
[7] Bykovetz N, Herman W N, Yuen T, Jee C S, Lin C L and Crow J E 1987 *J. Appl. Phys.* **61** 4355–7
[8] Yuen T, Lin C L, Crow J E and Bykovetz N 1992 *J. Magn. Magn. Mater.* **109** 98–102
[9] Begum R J, Nagarajan R and Gupta L C 1993 *Physica* B **186–188** 714–6
[10] Krylov V, Andreev A V, Sechovsky V and Havela L 1990 *Hyperfine Interact.* **59** 391–4
[11] Cottenier S, Demuynck S, Kaczorowski D, Spirlet J C, Meersschaut J and Rots M 1998 *J. Phys.: Condens. Matter* **10** 8381–7
[12] Sandratskii L M and Kübler J 1999 *Phys. Rev.* B **60** R6961–4
[13] Blaha P, Schwarz K and Luitz J 1999 *WIEN97, a Full Potential Linearized Augmented Plane Wave Package for Calculating Crystal Properties* Technische Universität Wien
[14] Schatz G and Weidinger A 1996 *Nuclear Condensed Matter Physics* (New York: Wiley)
[15] Barradas N P, Rots M, Melo A A and Soares J P 1993 *Phys. Rev.* B **47** 8763–8
[16] Hütten U, Vianden R and Kaufmann 1987 *Hyperfine Interact.* **34** 213–6
[17] Krishnamurthy V V, Mishra S N, Devare S H, Ramakrishnan S, Srinivas S and Chandra G 1990 *Hyperfine Interact.* **80** 1005–10
[18] Lawrence J M and Shapiro S M 1980 *Phys. Rev.* B **22** 4379–88
[19] Kohori Y, Inoue Y, Kohara T, Tomka G and Riedi P C 1999 *Physica* B **259–261** 103–4
[20] Heubes P, Korn D, Schatz G and Zibold G 1979 *Phys. Lett.* A **74** 267–70